Article
Chinese Science Bulletin
Molecular Biology
April 2012 Vol.57 No.11: 1280–1287
doi: 10.1007/s11434-012-4981-x

Kinetic study of the DNA annealing properties of RECQ5β helicase

DING XiuYan[1,2], XU YaNan[2], LI Wei[2], WANG PengYe[2], XI XuGuang[1,3] & DOU ShuoXing[2*]

[1] *College of Life Sciences, Northwest A&F University, Yangling 712100, China;*
[2] *Laboratory of Soft Matter Physics, Beijing National Laboratory for Condensed Matter Physics, Institute of Physics, Chinese Academy of Sciences, Beijing 100190, China;*
[3] *Institut Curie-Section de Recherche, Centre Universitaire, Bâtiment 110, F-91405 Orsay, France*

Received June 2, 2011; accepted November 11, 2011; published online February 23, 2012

RecQ family helicases are critical for maintaining genomic integrity. Many RecQ family helicases not only unwind duplex, and other more complicated DNA structures, but also possess, interestingly, DNA annealing (strand pairing) activity. Here, we systematically investigated the DNA annealing properties of RECQ5β by measuring DNA annealing kinetics, equilibrium DNA binding, and kinetics of dissociation from ssDNA. RECQ5β catalyzed DNA annealing most efficiently when the enzyme molecules covered approximately 40%–50% of the DNA strand, in the absence or presence of different nucleotide cofactors (AMPPNP, ATPγS, or ADP) under our buffer conditions. A comparative study with RECQ5β$^{1-662}$ confirmed that the C-terminal region of RECQ5β was essential for its high DNA annealing activity. These results contribute to our understanding of the mechanism of DNA annealing catalyzed by RecQ family helicases.

helicase, RECQ5β, DNA annealing, kinetics, DNA binding

Citation: Ding X Y, Xu Y N, Li W, et al. Kinetic study of the DNA annealing properties of RECQ5β helicase. Chin Sci Bull, 2012, 57: 1280–1287, doi: 10.1007/s11434- 012-4981-x

RecQ helicases are critical for the maintenance of genomic stability [1,2]. In humans, five family members, RECQ1 [3,4], BLM [5], WRN [6], RECQ4 [7] and RECQ5 [8], have been identified. Defects in BLM, WRN and RECQ4 lead to human hereditary disorders: Bloom syndrome, Werner syndrome and Rothmund-Thomson syndrome, respectively, which are characterized by genome instability and cancer predisposition [9].

Increasingly, studies have revealed that RecQ family helicases not only unwind duplex and other more complicated DNA structures, such as G4 DNA and Holliday junctions [10], but also possess DNA annealing (strand pairing) activity [11–14]. By combining DNA annealing activity with their inherent DNA unwinding capability, these enzymes may catalyze coordinated DNA strand exchange [12].

In humans, RECQ5 exists in three isoforms: RECQ5α, RECQ5β and RECQ5γ [8]. The three proteins are identical in their N-terminal regions (410 residues) and all contain the seven conserved helicase motifs. In addition to the helicase core, RECQ5β contains a putative RQC domain, which is followed by a long C-terminal region that appears to be dissimilar to the other RecQ family helicases. Previously, biochemical studies showed that RECQ5β has both DNA unwinding and annealing activities, with the latter residing in the C-terminal region of the helicase [11]. In addition, the annealing activity may be inhibited by the non-hydrolyzable ATP analog, ATPγS, by an unknown mechanism [11]. The annealing activity may be partially inhibited by ADP [15]. At present, the molecular mechanism underlying the DNA annealing activity of RECQ5β and other RecQ family helicases remains unclear.

In this work, as an essential step towards the better understanding of DNA annealing behaviors of RECQ5β helicase, we studied the effects of enzyme concentration and nucleotide cofactors on its DNA annealing kinetics. In addition, we also performed equilibrium DNA binding and kinetic dissociation assays. Finally, as a comparison, we per-

*Corresponding author (email: sxdou@iphy.ac.cn)

formed similar measurements for a truncation mutant of the helicase, RECQ5β$^{1-662}$.

1 Materials and methods

1.1 Reagents and buffers

All chemicals were of reagent grade and all solutions were prepared in high quality de-ionized water from a Milli-Q water purification system (Millipore Corporation, France) having a resistance greater than 18.2 MΩ cm. All DNA annealing, ssDNA binding, and dissociation assays were performed in a buffer comprising 25 mmol L^{-1} Tris-HCl, pH 7.5 (25°C), 10 mmol L^{-1} NaCl, 1.5 mmol L^{-1} $MgCl_2$ and 0.1 mmol L^{-1} dithiothreitol (DTT), at 37°C, unless otherwise mentioned in the text.

1.2 RecQ protein and oligonucleotide substrates

RECQ5β protein was expressed and purified as previously described [15]. The 45-nt complementary ssDNA substrates used in the annealing assay were labeled with fluorescein (F) and hexachlorofluorescein (H), respectively. Their structures and sequences were 5'-AGATCCCTCAGACCCTTTTAGTCAGTGTGGAAAATCTCTAGCAGT-F-3' and 5'-H-ACTGCTAGAGATTTTCCACACTGACTAAAAGGGTCTGAGGGATCT-3'. The 20-nt ssDNA used in the DNA binding and dissociation assays was labeled with fluorescein. Its structure and sequence was 5'-TTTGGCGACGGCAGCGAGGC-F-3'. The protein trap used in the dissociation assay was 56-nt poly(dT), dT_{56}. All the single-stranded oligonucleotides, with or without labels, were purchased from the Shanghai Sangon Biological Engineering Technology & Services Co., Ltd, and all the synthetic oligonucleotides were purified by high-performance liquid chromatography. The dsDNA used for calibration of annealing efficiency was prepared by mixing equal concentrations (50 μmol L^{-1}) of complementary single-stranded oligonucleotides in a 20 mmol L^{-1} Tris-HCl buffer (pH 8.0 at 25°C) containing 100 mmol L^{-1} NaCl, followed by heating to 90°C. After equilibrating for 3 min, annealing proceeded by slow cooling to room temperature.

1.3 Kinetics assay for DNA strand annealing

The stopped-flow DNA annealing assay based on FRET (fluorescence resonance energy transfer) was performed similarly to that described previously [15]. Briefly, the experiment was carried out using a Bio-logic SFM-400 mixer with a 1.5 mm×1.5 mm cell (FC-15, Bio-Logic, France) and a Bio-Logic MOS450/AF-CD optical system equipped with a 150-W mercury-xenon lamp. The reaction was performed in the two-syringe mode, where 2-nmol L^{-1} F-labeled complementary ssDNA and half of the helicase solution were pre-incubated in syringe #1 while 2-nmol L^{-1} H-labeled complementary ssDNA and the other half of the helicase solution were pre-incubated in syringe #4, respectively, in the reaction buffer. The reaction was initiated by rapidly mixing the two syringes. The sample was excited at 492 nm and the fluorescence signal was monitored at 525 nm.

For converting the output data from volts to percent annealing, we performed another experiment in two-syringe mode, where the helicase was in syringe #1, and the pre-annealed dsDNA was in syringe #4. The fluorescent signal of the mixed solution from the two syringes corresponded to 100% annealing. The reaction was carried out at 37°C.

1.4 Anisotropy assay for equilibrium DNA binding

DNA binding of RECQ5β was analyzed by fluorescence polarization, as described previously [15]. The assay was performed using a Bio-Logic auto-titrator (TCU-250) and the Bio-Logic optical system (MOS450/AF-CD) in fluorescence anisotropy mode. Varying amounts of protein were added to 1 mL of binding buffer containing 8 nmol L^{-1} 20-nt F-labeled ssDNA substrate. Each sample was allowed to equilibrate in solution for 1.5 min, after which fluorescence polarization was measured. Titrations were performed in a temperature-controlled cuvette at 37°C. The solution was continuously stirred by a small magnetic stir bar during the whole titration process.

1.5 Anisotropy assay for dissociation kinetics of RECQ5β from ssDNA

The anisotropy assay for dissociation kinetics of RECQ5 from ssDNA was performed as described previously [16]. We used the Bio-Logic SFM-400 stopped-flow mixer and the Bio-Logic MOS450/AF-CD optical system operating in anisotropy mode. In this assay, the helicase, with or without nucleotide cofactors, was pre-incubated with F-labeled 20-nt ssDNA substrate in one syringe while the protein trap (dT_{56}) was in another syringe. The reaction was initiated by rapid mixing of the two syringes. The sample was excited at 492 nm and the anisotropy was monitored at 525 nm. Upon initiation, the helicase dissociated from the substrate and was trapped by the protein trap, resulting in a decay of anisotropy.

2 Results and discussion

2.1 Real-time observation of DNA annealing based on FRET

Fluorometric assays have frequently been used in studies of DNA unwinding and the DNA binding properties of helicases. Previously, we used a FRET-based fluorometric assay to observe, in real time, DNA unwinding and annealing behaviors of helicases [15,17]. The principle of the

FRET-based fluorometric DNA annealing assay is as follows.

One ssDNA strand was labeled with fluorescein at the 3' end, whereas a complementary ssDNA strand was labeled with hexachlorofluorescein at the 5' end. As there is a large spectrum overlap between the fluorescein emission and hexachlorofluorescein excitation spectra [17], after annealing and formation of dsDNA, the fluorescein and hexachlorofluorescein are in close proximity and FRET will occur between the two fluorescent molecules. As a result, the fluorescence emission of fluorescein (peaking at 525 nm) becomes reduced and that of hexachlorofluorescein (peaking at 556 nm) enhanced. By monitoring the fluorescence signal change at 525 nm, the DNA annealing kinetics can be measured.

Figure 1(a) shows a typical DNA annealing kinetic course for two complementary 45-nt ssDNA in the presence of 15 nmol L^{-1} RECQ5β helicase. Also shown in this figure is the calibration curve for 100% annealing, which was obtained by mixing pre-annealed 45-bp dsDNA and RECQ5β at the same concentrations as in the annealing measurement. After normalization of the annealing data curve using an average value from the calibration curve, the time course of DNA annealing efficiency was obtained (Figure 1(b)).

2.2 Kinetics of RECQ5β-catalyzed DNA annealing in the absence or presence of different cofactors

In previous studies of DNA annealing behaviors of RECQ5β, it was found that the annealing efficiency depended on the nucleotide state, for unknown reasons [11,15]. In particular, the non-hydrolyzable ATP analogue, ATPγS, almost completely inhibited the RECQ5β-catalyzed DNA annealing. In addition, it was found that the annealing efficiency also depended on the enzyme concentration.

To better understand these observed phenomena, we systematically studied the kinetics of RECQ5β-catalyzed DNA annealing with the FRET-based DNA annealing assay described above. First, we studied the annealing kinetics of RECQ5β in the apo (nucleotide-free) state. Figure 2 shows

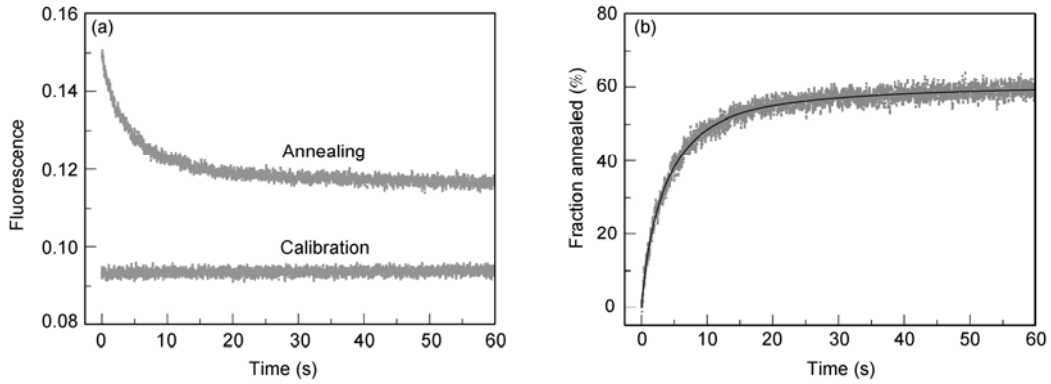

Figure 1 FRET-based fluorometric assay for ssDNA annealing kinetics. (a) Annealing was measured by monitoring the decrease of the fluorescent signal of fluorescein at 525 nm in real time. The annealing reaction was initiated by mixing 2 nmol L^{-1} F-labeled 45-nt DNA, 2 nmol L^{-1} H-labeled 45-nt complementary DNA, each pre-incubated with 7.5 nmol L^{-1} RECQ5β. The calibration curve for 100% annealing was obtained by mixing 2 nmol L^{-1} pre-annealed 45-bp dsDNA and 15 nmol L^{-1} RECQ5β (see Materials and Methods). All concentrations indicated are final reaction concentrations. (b) The time course of DNA annealing efficiency was obtained by normalizing the annealing data curve in (a) using the average value of the calibration curve, 0.093. The solid line represents a triple-exponential fit of the data curve.

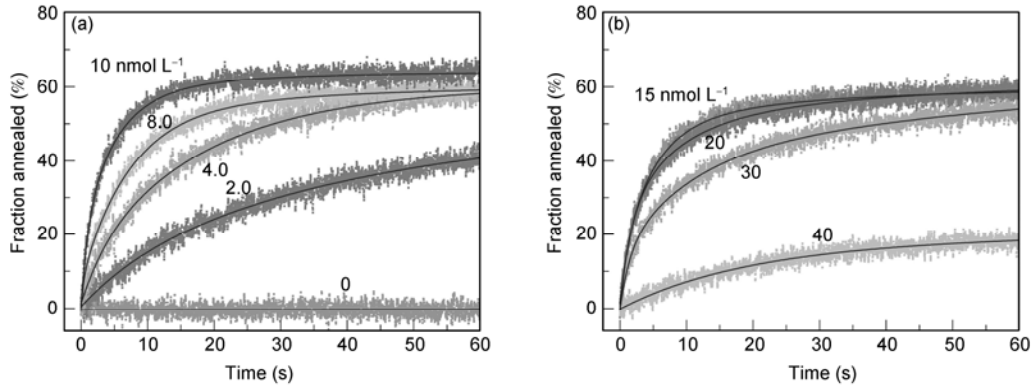

Figure 2 Typical time courses of ssDNA annealing catalyzed by RECQ5β (in the apo state) at different enzyme concentrations. The measurements were carried out under the same conditions as in Figure 1, except for the enzyme concentration. The solid lines represent double-exponential fits of the data curves in the cases of slow annealing (0, 2, 4, 40 nmol L^{-1}), and triple-exponential fits in the other cases of quick annealing. The initial annealing rates obtained from the fits are given in Figure 3.

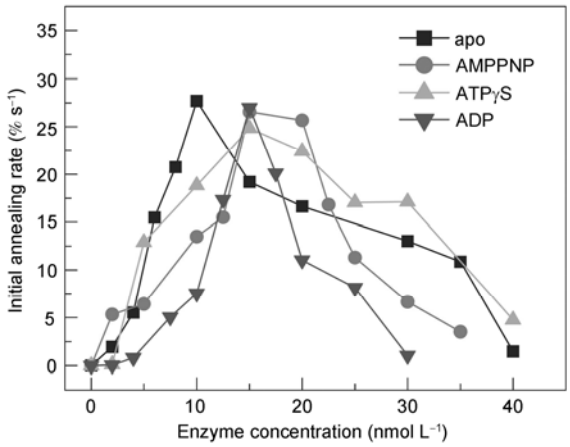

Figure 3 Initial rate of DNA annealing catalyzed by RECQ5β in different nucleotide states. All the measurements were carried out under the same conditions, except for the nucleotide cofactors (0.1 mmol L^{-1}). The rates were obtained from exponential fitting of the annealing kinetic data curves.

some typical annealing data curves at different enzyme concentrations. By double- or triple-exponential fits of the data curves, we obtained the initial annealing rate at each enzyme concentration. The results are given in Figure 3. Note that the annealing of ssDNA in the absence of RECQ5β is negligible over the short time range that is shown.

Then, to determine the effect of nucleotide cofactors, we performed similar measurements in the presence of ADP or the non-hydrolyzable ATP analogues, AMPPNP or ATPγS (data not shown). AMPPNP has not been used in annealing studies before, and we wanted to know whether it has the same effect as ATPγS.

After data analyses, the initial annealing rates in the presence of different nucleotide cofactors were obtained and are shown in Figure 3.

From Figure 3, we could observe several interesting properties of RECQ5β-catalyzed DNA annealing. (i) There is an optimum enzyme concentration, between 10 and 20 nmol L^{-1}, for DNA annealing in each case. (ii) All the maximum initial annealing rates are quite similar for the four different cases, which seems to contradict the previous observation that ATPγS and ADP inhibit the annealing activity of RECQ5β [11,15]. This will be discussed later. (iii) RECQ5β efficiently catalyzes DNA annealing over a wide range of concentration in the apo and ATPγS states, but over a much narrower range in the case of ADP.

If we define an efficient enzyme concentration range in which the initial annealing rate is higher than half of the maximum value, then we can obtain this parameter for each case from Figure 3. They are 5.6–27.7, 9.8–24.1, 4.9–33.8, and 11.5–19.3 nmol L^{-1} for the cases of apo, AMPPNP, ATPγS, and ADP, respectively. These data will be used later for estimating the extent of coverage of ssDNA by the enzyme when efficient annealing occurs.

2.3 Equilibrium ssDNA binding of RECQ5β

It may be queried why there is an optimum enzyme concentration for DNA annealing. To answer this question, we performed equilibrium DNA binding experiments using the anisotropy assay. By titrating F-labeled 20-nt ssDNA with RECQ5β and measuring the fluorescence anisotropy, we obtained data curves for equilibrium DNA binding of the enzyme in different nucleotide states (Figure 4). Clearly, in each case, the anisotropy first increases with increasing enzyme concentration, and then, at high enzyme concentrations, the anisotropy saturates. As the anisotropy reflects the extent to which the ssDNA is covered with bound enzyme molecules, the data curves indicate that the ssDNA molecule is partially covered with the enzyme at low concentrations and completely covered with the enzyme at high concentrations for each case of nucleotide cofactor. Note that we used 20-nt rather than 45-nt ssDNA in the binding measurement. For a direct comparison with the preceding annealing results, where a total of 4 nmol L^{-1} 45-nt ssDNA was used, here we used a doubled ssDNA concentration of 8 nmol L^{-1}.

From the efficient enzyme concentration range given previously and the DNA binding data curves in Figure 4, we found that efficient annealing occurs when the coverage of ssDNA by the enzyme is in the range of 39.4% ± 22.8% (apo), 37.3% ± 14.0% (AMPPNP), 37.8% ± 26.3% (ATPγS), or 49.1% ± 9.9% (ADP).

Surprisingly, the central values of these ranges (39.4%, 37.3%, 37.8% and 49.1%) are quite similar, especially for the three cases of apo, AMPPNP, and ATPγS. This indicates that RECQ5β-catalyzed DNA annealing proceeds optimally at levels of enzyme sufficient to cover approximately 40%–50% of the DNA strand, regardless of the nucleotide state. When the enzyme concentration is higher, such that the ssDNA is covered by more enzyme molecules, the annealing efficiency becomes reduced. We think this is

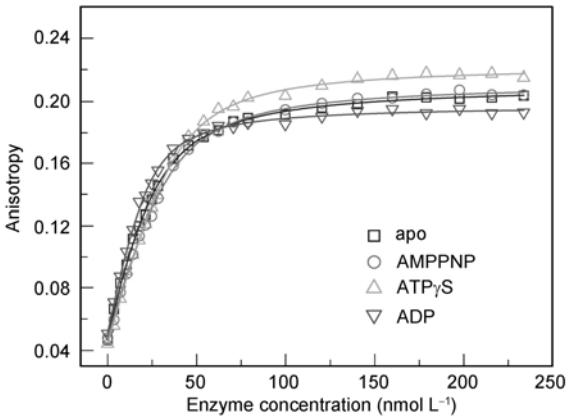

Figure 4 Equilibrium DNA-binding activities of RECQ5β in different nucleotide states. The anisotropy-based binding curves were obtained by titrating 8 nmol L^{-1} F-labeled 20-nt ssDNA with increasing RECQ5β, in the absence or presence of 0.1 mmol L^{-1} nucleotide cofactors (see Materials and methods).

quite reasonable: if the ssDNA is covered with too many enzyme molecules, the probability of the two complementary ssDNA strands to contact and form base pairs would be diminished.

Interestingly, recA-catalyzed ssDNA annealing occurs optimally at protein levels below that required to saturate the DNA strands, and saturating amounts of recA protein significantly reduced the rate of reaction [18], which is similar to our observations for RECQ5β. By nuclease protection analysis, the authors showed that recA only covered 10%–15% of the ssDNA at the optimal protein concentration for annealing.

2.4 Dissociation kinetics of RECQ5β from ssDNA

As already mentioned, previous studies of the DNA annealing behaviors of RECQ5β revealed that the annealing efficiency depended on the nucleotide state [11,15]. We think this probably results from the varying affinities for ssDNA of the enzyme in the different nucleotide states. As the catalysis of DNA annealing relies on the binding of the enzyme to ssDNA, it is easy to imagine that annealing cannot be efficient if the affinity of the enzyme for ssDNA is too low or too high. At a normal enzyme concentration, if the affinity is too low, the ssDNA would be essentially free from bound enzyme and DNA annealing could not be catalyzed. Conversely, if it is too high, the bound enzyme molecules would not detach from the ssDNA and the annealing of two complementary ssDNA molecules could not proceed either.

To determine the affinities of the enzyme for ssDNA in different nucleotide states, we used a fluorescence polarization anisotropy assay to measure the dissociation kinetics of bound RECQ5β helicase from ssDNA in the presence of different nucleotide cofactors. We used a 20-nt fluorescein-labeled ssDNA as the substrate. This substrate was the same as that used for equilibrium DNA binding. We observed that the dissociation of RECQ5β from this substrate exhibited similar behaviors under the different conditions of apo, AMPPNP, and ATPγS: there were two phases: a slow one and a fast one (Figure 5(a)). The slow phase should describe the actual dissociation process of the helicase from the ssDNA. The fast phase may correspond to the dissociation process of helicase monomers that were bound less tightly to the two ends of the ssDNA [16]. In the case of the ADP state, there is only one phase.

For clarity, Figure 5(b) shows the dissociation rates in the four cases (in the cases of apo, AMPPNP and ATPγS, only the slow-phase rates were given). From these data it can be observed that the helicase binds to the ssDNA substrate most tightly in the ATPγS state and most weakly in the ADP state. The helicase has similar affinities for ssDNA in the apo and AMPPNP states.

2.5 RECQ5β-catalyzed annealing of non-complementary ssDNA

As mentioned before, the maximum initial annealing rates were quite similar for all the different nucleotide states in our experiments, while previous observations showed that ATPγS and ADP inhibited the annealing activity of RECQ5β [11,15]. This discrepancy is rather puzzling but one possible reason may be the different experimental methods. In the previous work, the annealing reaction products were analyzed directly by nondenaturing polyacrylamide gel electrophoresis. In our present work, however, the annealing processes were indirectly measured by monitoring the fluorescence signal changes. Thus, there is the possibility that the fluorescence signal change in our assay simply resulted from the gathering of ssDNA molecules with the aid of RECQ5β, rather than real duplex formation. That is, what we have observed may be not real

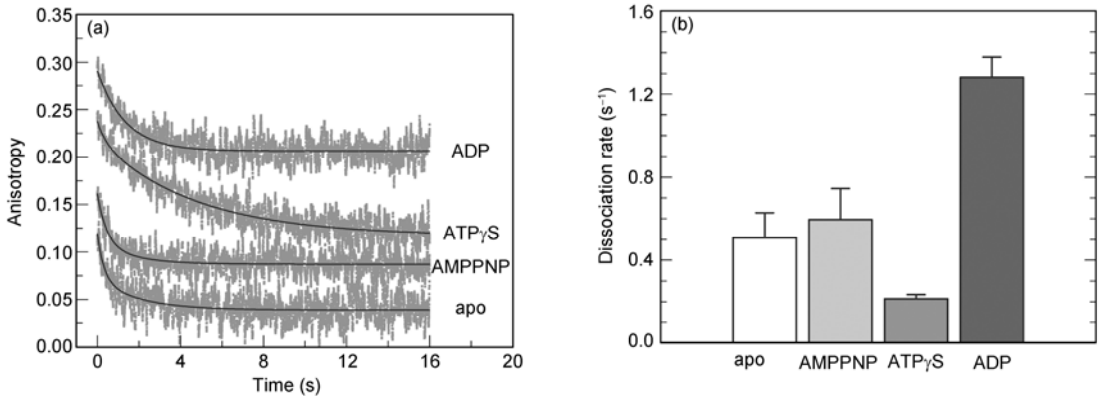

Figure 5 Dissociation kinetics of bound RECQ5β from ssDNA substrate in the absence or presence of nucleotide cofactors. (a) Kinetic time courses. 10 nmol L^{-1} F-labeled 20-nt ssDNA substrate was pre-incubated, in the absence or presence of 0.1 mmol L^{-1} nucleotide cofactors, with 100 nmol L^{-1} RECQ5β in reaction buffer at 37°C for 5 min, and the reaction was initiated by adding 2 μmol L^{-1} protein trap (dT_{56}) (see Materials and methods). The solid lines are single-(ADP) or double-exponential fits (apo, AMPPNP, and ATPγS) of the data. (b) Rates of the helicase dissociation from ssDNA substrate obtained from the above exponential fits. In cases of a biphasic dissociation process, only the relevant slow-phase rate is shown.

DNA annealing. To clarify this issue, we performed annealing kinetic assays using non-complementary F- and H-labeled ssDNA substrates. If the above conjecture was correct, then we would observe similarly significant fluorescence signal changes as those observed while using complementary ssDNA substrates.

As a control, an annealing assay using complementary ssDNA substrates was also carried out under the same conditions. From Figure 6 it can be seen that, in the cases of both apo and ATPγS, the fluorescence signal change for non-complementary substrates is much smaller than that for complementary substrates. This clearly demonstrates that our previous observations reflected the real ssDNA annealing properties of RECQ5β.

2.6 Inhibition of RECQ5β-catalyzed annealing by ATPγS in another reaction buffer

The above discrepancy is very probably caused by the different reaction buffers used. In the previous studies [11,15], the annealing buffer used was 20 mmol L^{-1} Tris-acetate, pH 7.9, 50 mmol L^{-1} KOAc, 10 mmol L^{-1} $Mg(OAc)_2$, 1 mmol L^{-1} DTT, and 50 mg mL^{-1} BSA. In our current fluorometric assay, the buffer is 25 mmol L^{-1} Tris-HCl, pH 7.5 (25°C), 10 mmol L^{-1} NaCl, 1.5 mmol L^{-1} $MgCl_2$, and 0.1 mmol L^{-1} DTT. Our buffer was chosen because of its good performance in RECQ5β-catalyzed dsDNA unwinding, and we thought it would be more insightful to study the annealing and unwinding properties of the helicase under the same buffer conditions. Considering that the interaction between an enzyme and DNA is usually sensitive to buffer conditions, our suggestion for the cause of the discrepancy appears reasonable.

To verify the above proposal, we then performed annealing kinetic assays with the reaction buffer used in the previous studies [11,15]. The results are shown in Figure 7. It can be seen that ATPγS obviously reduced the magnitude of fluorescence signal change (by approximately 50%). That is, ATPγS indeed inhibited the annealing activity of RECQ5β in the different reaction buffer, as expected. It should be noted that ATPγS did not completely inhibit annealing. In the previous studies, ATPγS-mediated inhibition was also not complete, despite being more significant than that observed here [11,15].

So why is the annealing activity of RECQ5β inhibited by ATPγS and ADP under the previous studies' buffer conditions [11,15]? Although our dissociation results (Figure 5) were obtained using a buffer that was different from their annealing buffer, they should be still useful for understanding the different effects of nucleotide cofactors on RECQ5β-catalyzed ssDNA annealing. As the binding affinity of the helicase for ssDNA is modulated by the nucleotide cofactor [16], we think the reason for the observed inhibition effects is that RECQ5β binds to ssDNA too tightly in the ATPγS state and too loosely in ADP state. Interestingly, it has been observed that *Drosophila* RecQ4 helicase, another member of RecQ family, forms a stable complex with ssDNA in the presence of AMPPNP and has a reduced annealing activity [19]. The presence of ADP, however, does not affect either the affinity for ssDNA or the ssDNA annealing efficiency of RecQ4. Thus, these observations also imply a close correlation between ssDNA binding and the annealing properties of the helicases.

2.7 DNA annealing catalyzed by RECQ5β$^{1-662}$

Garcia et al. [11] found that the DNA annealing activity of RECQ5β resides in its C-terminal region. To verify this conclusion, we studied the annealing kinetics of a C-terminal truncation mutant of RECQ5β, RECQ5β$^{1-662}$, in the apo state. The initial annealing rate as a function of enzyme concentration is given in Figure 8(a). By comparing this result with that in Figure 3, it is immediately obvious that the maximum initial annealing rate (approximately 3% s^{-1})

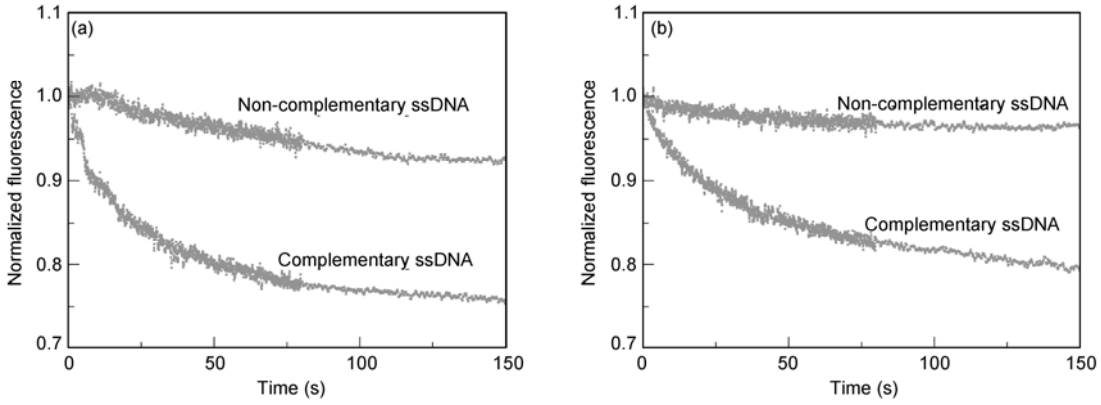

Figure 6 Comparison of the DNA annealing behaviors of RECQ5β (40 nmol L^{-1}) with complementary and non-complementary ssDNA. The experiments were performed under the same conditions as in Figure 1(a), except for the enzyme concentration. In the case of non-complementary ssDNA, the structure and sequence of the H-labeled 45-nt ssDNA is 5′-H-AATCCGTCGAGCAGAGTTTTTTTTTTTTTTTTTTTTTTTTTTTTT-3′. (a) No nucleotide cofactor (apo state); (b) ATPγS (0.1 mmol L^{-1}) is present.

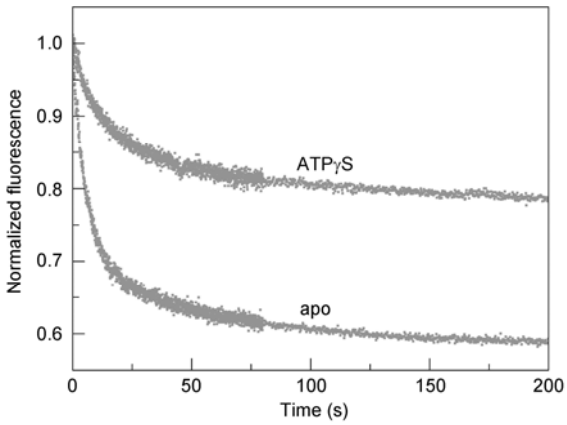

Figure 7 DNA annealing behaviors of RECQ5β (40 nmol L^{-1}) with complementary ssDNA in the absence or presence of ATPγS (0.1 mmol L^{-1}), with an annealing buffer the same as that used in the previous studies [11,15] (i.e., 20 mmol L^{-1} Tris-acetate, pH 7.9, 50 mmol L^{-1} KOAc, 10 mmol L^{-1} $Mg(OAc)_2$, 1 mmol L^{-1} DTT, 50 mg/ml BSA). The experiments were performed under the same conditions as in Figure 1(a), except for the enzyme concentration.

is significantly (by about one order of magnitude) lower than that of RECQ5β. From Figure 8(a), the efficient enzyme concentration range is obtained for RECQ5β$^{1-662}$, 4.6–16.3 nmol L^{-1}.

For comparison with the full-length RECQ5β, we also performed equilibrium DNA binding and kinetic dissociation assays for RECQ5β$^{1-662}$ in the apo state (Figure 8(b) and (c)). With the DNA binding data curve, we observed that efficient annealing occurs when the coverage of ssDNA by RECQ5β$^{1-662}$ is in the range of 52.9% ± 23.3%, indicating that the RECQ5β$^{1-662}$-catalyzed DNA annealing also proceeds optimally when the helicase covers about half of the DNA strand, as for the full-length enzyme. It would be interesting to see if this observed feature is equally applicable to other RecQ family helicases in future studies.

As in the case of RECQ5β, the dissociation of RECQ5β$^{1-662}$ from ssDNA occurred in two phases: a slow one and a fast one. The slow phase rate was (0.45 ± 0.04) s^{-1}, almost the same as that of RECQ5β in the apo state ((0.51 ± 0.12) s^{-1}). Note that, although RECQ5β and RECQ5β$^{1-662}$ have almost the same affinity for ssDNA, the two enzymes have significantly different DNA annealing efficiencies. This indicates that the annealing abilities of certain helicases, such as RECQ5β, do not simply result from their ssDNA binding behavior alone, but rather, it is an intrinsic property of these helicases that should be determined by their specific structures. In the case RECQ5β, the C-terminal region is indeed mainly responsible for its DNA annealing activity, as previously noted [11].

3 Conclusion

In this study we systematically studied the DNA annealing

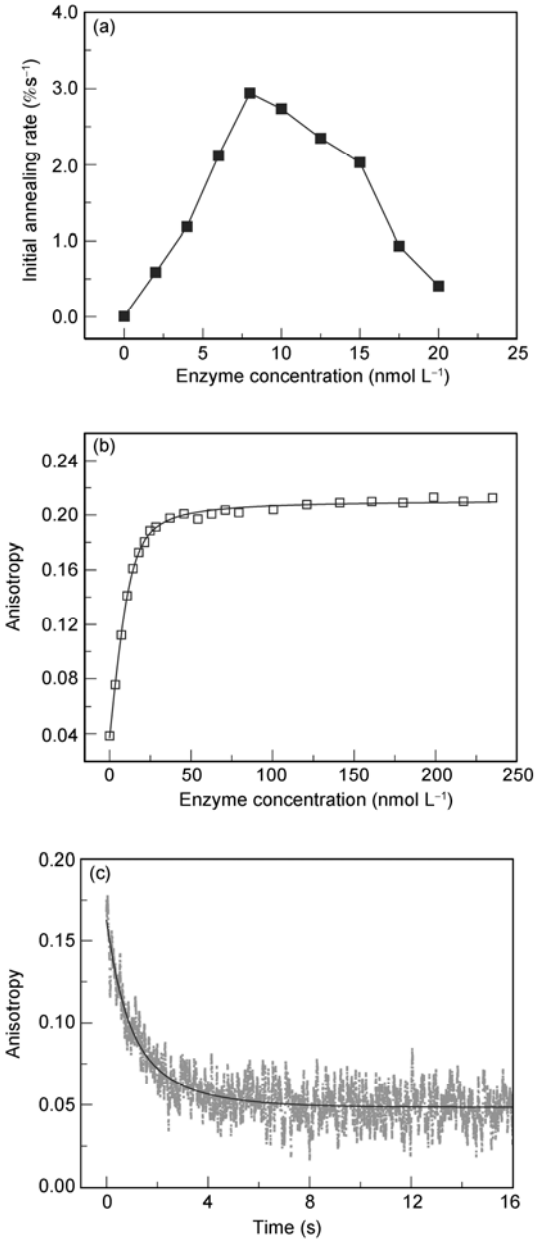

Figure 8 DNA annealing, DNA binding, and dissociation behaviors of RECQ5β$^{1-662}$. (a) Initial rate of DNA annealing catalyzed by RECQ5β$^{1-662}$ in the apo state. The measurement was carried out under the same conditions as for RECQ5β in Figure 2. (b) Equilibrium DNA binding activity of RECQ5β$^{1-662}$ in the apo state. The measurement was carried out under the same conditions as for RECQ5β in Figure 4. (c) Dissociation kinetic curve of bound RECQ5β$^{1-662}$ using 20-nt ssDNA substrates in the absence of nucleotide cofactors, obtained under the same conditions as for RECQ5β in Figure 5. The solid line is a double-exponential fit of the data, giving a slow phase rate of 0.45 ± 0.04 s^{-1}.

properties of RECQ5β by measuring DNA annealing kinetics, equilibrium DNA binding, and kinetics of dissociation from ssDNA.

By combining the experimental results obtained from DNA annealing kinetics and equilibrium DNA binding assays, we showed, for the first time, that RECQ5β-catalyzed

DNA annealing most efficiently when the enzyme concentration is at a level to cover about half of the DNA strand, regardless of nucleotide cofactors. This phenomenon is likely to be closely related to the mechanism of DNA annealing by the helicase.

We observed that the annealing activity of RECQ5β is not inhibited by ATPγS and ADP, using our reaction buffer. Inhibition of the annealing activity of RECQ5β by ATPγS and ADP as observed previously under different buffer conditions [11,15] was probably due to modulations of the ssDNA binding affinity of the enzyme by the two nucleotide cofactors. A comparative study with RECQ5β$^{1-662}$ revealed that the annealing ability of the enzyme is not simply caused by its ssDNA binding capability alone, and that the C-terminal region of RECQ5β is indeed essential for efficiently catalyzing DNA annealing.

The experimental observations in the present work contribute to the further understanding of the mechanism of DNA annealing catalyzed by the RecQ family helicases. Although it is believed that the DNA annealing activities of the RecQ family helicases are implicated in their cellular functions, the molecular basis for these activities is currently unclear. In particular, it is still not known whether oligomerization of these enzymes is required for catalyzing DNA annealing. We believe that, by combining biochemical, biophysical and structural studies, the underlying mechanism for DNA annealing will be gradually elucidated.

This work was supported by the National Natural Science Foundation of China (10834014) and the National Basic Research Program of China (2009CB930704).

1 Hickson I D. RecQ helicases: Caretakers of the genome. Nat Rev Cancer, 2003, 3: 169–178
2 Mankouri H W, Hickson I D. Understanding the roles of RecQ helicases in the maintenance of genome integrity and suppression of tumorigenesis. Biochem Soc Trans, 2004, 32: 957–958
3 Puranam K L, Blackshear P J. Cloning and characterization of RECQL, a potential human homologue of the *Escherichia coli* DNA helicase RecQ. J Biol Chem, 1994, 269: 29838–29845
4 Seki M, Miyazawa H, Tada S, et al. Molecular cloning of cDNA encoding human DNA helicase Q1 which has homology to *Escherichia coli* RecQ helicase and localization of the gene at chromosome 12p2. Nucleic Acids Res, 1994, 22: 4566–4573
5 Ellis N A, Groden J, Ye T Z, et al. The Bloom's syndrome gene product is homologous to RecQ helicases. Cell, 1995, 83: 655–666
6 Yu C E, Oshima J, Fu Y H, et al. Positional cloning of the Werner's syndrome gene. Science, 1996, 272: 258–262
7 Kitao S, Ohsugi I, Ichikawa K, et al. Cloning of two new human helicase genes of the RecQ family: Biological significance of multiple species in higher eukaryotes. Genomics, 1998, 54: 443–452
8 Shimamoto A, Nishikawa K, Kitao S, et al. Human RecQ5β, a large isomer of RecQ5 DNA helicase, localizes in the nucleoplasm and interacts with topoisomerases 3α and 3β. Nucleic Acids Res, 2000, 28: 1647–1655
9 Karow J K, Wu L, Hickson I D. RecQ family helicases: Roles in cancer and aging. Curr Opin Genet Dev, 2000, 10: 32–38
10 Bennett R J, Keck J L. Structure and function of RecQ DNA helicases. Crit Rev Biochem Mol Biol, 2004, 39: 79–97
11 Garcia P L, Liu Y, Jiricny J, et al. Human RECQ5β, a protein with DNA helicase and strand-annealing activities in a single polypeptide. EMBO J, 2004, 23: 2882–2891
12 Machwe A, Xiao L, Groden J, et al. RecQ family members combine strand pairing and unwinding activities to catalyze strand exchange. J Biol Chem, 2005, 280: 23397–23407
13 Sharma S, Sommers J A, Choudhary S, et al. Biochemical analysis of the DNA unwinding and strand annealing activities catalyzed by human RECQ1. J Biol Chem, 2005, 280: 28072–28084
14 Cheok C F, Wu L, Garcia P L, et al. The Bloom's syndrome helicase promotes the annealing of complementary single-stranded DNA. Nucleic Acids Res, 2005, 33: 3932–3941
15 Ren H, Dou S X, Zhang X D, et al. The zinc-binding motif of human RECQ5β suppresses the intrinsic strand-annealing activity of its DExH helicase domain and is essential for the helicase activity of the enzyme. Biochem J, 2008, 412: 425–433
16 Yang Y, Dou S X, Xu Y N, et al. Kinetic mechanism of DNA unwinding by the BLM helicase core and molecular basis for its low processivity. Biochemistry, 2010, 49: 656–668
17 Zhang X D, Dou S X, Xie P, et al. RecQ helicase-catalyzed DNA unwinding detected by fluorescence resonance energy transfer. Acta Biochim Biophys Sin, 2005, 37: 593–600
18 Bryant F R, Lehman I R. On the mechanism of renaturation of complementary DNA strands by the recA protein of *Escherichia coli*. Proc Natl Acad Sci USA, 1985, 82: 297–301
19 Capp C, Wu J, Hsieh T S. *Drosophila* RecQ4 has a 3'-5' DNA helicase activity that is essential for viability. J Biol Chem, 2009, 284: 30845–30852